Canadian Prairie Rangeland and Seeded Forage Classification Using Multiseason Landsat 8 and Summer RADARSAT-2 ☆

Emily J. Lindsay [a,b,*], Douglas J. King [a], Andrew M. Davidson [a,b], Bahram Daneshfar [b]

[a] Carleton University, Department of Geography and Environmental Studies, Ottawa, ON K1S 5B6, Canada
[b] Agriculture and Agri-Food Canada, Earth Science and Technology Branch, Ottawa, ON K1A 0C5, Canada

ARTICLE INFO

ABSTRACT

Rangeland and seeded forage in Canada's Prairie provinces represent productive landscapes that provide multiple ecosystem services. Past efforts to map these resources at regional scales have not achieved consistently high accuracies as they are spatially variable in both ecology and management. In particular, Agriculture and Agri-food Canada needs to distinguish these land use classes from each other and from cropland in its annual national agricultural land cover inventory. Given the potential to distinguish these classes based on seasonal phenological differences, this study used multi-season Landsat 8 top-of-atmosphere reflectance data and derived vegetation and phenological indices, as well as mid-summer RADARSAT-2 data in random forest classification of two ecoregions in Alberta and Manitoba. Classification accuracy was compared for single and multi-date Landsat 8 variables, the vegetation index and phenological variable groups, RADARSAT-2 VV and VH backscatter intensity, and combined datasets. Variable importance analysis showed that spring Landsat 8 reflectance generally contributed most to class discrimination, but accuracy improved with the addition of Landsat 8 data from the other seasons. Vegetation indices and phenological variables produced similar accuracies and were deemed to not warrant the additional processing effort to derive them. RADARSAT-2 VH backscatter was the most important variable for the Manitoba study area, which is wetter with more vegetation structure variability than the Alberta study area. Backscatter intensity significantly increased overall accuracy when it was combined with one or two-season Landsat 8 data. The best overall accuracy was achieved using the three seasons of Landsat 8 and mid-summer RADARSAT-2 data, but it was not significantly better than that for two season Landsat 8 + RADARSAT-2. The methods presented in this paper provide a process for accurate and efficient classification of seeded forage, rangeland and cropland that can be applied over large areas in operational agricultural land cover inventory.

Crown Copyright © 2018 Published by Elsevier Inc. on behalf of The Society for Range Management. All rights reserved.

Introduction

Range and seeded forage lands are important in many regions of the world to the grazing/meat production industry and in supporting multiple ecological functions and services. They provide soil conservation (Fox et al., 2012), carbon and water storage (Wang et al., 2014), and important habitat for supporting plant and animal biodiversity (Fuhlendo Random Forest et al., 2012), including many bee species critical for pollination services (Sheffield et al., 2014). Vegetation dynamics on native prairie grasslands are a function of grazing, climate, fire, and soil type and condition (Bailey and Bailey, 1994).

Rangeland is commonly not seeded and comprises mostly native species while seeded forage is dominated by plants that are seeded for livestock consumption. In Canada, seeded forage is generally more intensively managed than rangeland and includes land that is grazed (pasture) or harvested (hay). Some plant species are used in both pasture and hay, which renders spectral discrimination of these two land cover types difficult, particularly from space-based platforms. For the purposes of this study, these two types are considered together as a single seeded forage class defined as mechanically planted perennial grass and legume mixtures for grazing or harvesting for livestock fodder. Seeded forage and rangeland occur primarily in the Canadian Prairies (Fig. 1), which extend across the southern portions of three provinces: Alberta, Saskatchewan, and Manitoba. Ecologically, these areas are commonly classified on the basis of four main plant community associations: aspen parkland, fescue prairie, tallgrass, and mixed prairie (Ecological Stratification Working Group, 1995).

Accurate estimates of the spatial distribution of native rangeland are necessary to monitor, manage, and conserve this resource from further landscape fragmentation due to expanded annual crop production, natural resource extraction, and settlement expansion, as well as to

understand its role in provision of habitat for species at risk (Roch and Jaeger, 2014). An Earth observation-based agricultural inventory that is produced annually by Agriculture and Agri-food Canada (AAFC) achieves a target of 85% overall mapping accuracy for the agricultural (crop) classes in the Prairie provinces (Fisette et al., 2014; Davidson et al., 2017). However, to date, such high accuracies for the rangeland and seeded forage classes in this data product have not been attained due to confusion with each other and with cropland (Fisette et al., 2014). The diversity of vegetation species in seeded forage and rangeland is high (Ali et al., 2016), regionally variable (Hall-Beyer, 2012), and often augmented by invasive species (DiTomaso, 2000), resulting in overlap in their reflectance distributions and with cropland reflectance at optical satellite-image scales (Wu and Li, 2009). Alternatively, Synthetic Aperture Radar (SAR) backscatter has been used to distinguish cropland from pasture and forage, with greatest accuracy being achieved in late summer, when the structural differences between crops and pasture are greatest (McNairn et al., 2009), while crop types have been classified using late summer to early fall imagery acquired after wheat harvest (Deschamps et al., 2012). Discrimination of native grassland/rangeland from seeded forage or other types of modified grassland is more difficult, but Smith and Buckley (2011) had some success using midsummer July SAR imagery.

The use of vegetation indices and texture variables derived from optical data has improved grassland classification performance (Smith et al., 2015; Yang et al., 2017) and biophysical modeling of rangeland characteristics (Yang et al., 2012; Jansen et al., 2016). Multitemporal optical (McInnes et al., 2015; Yang et al., 2017) or SAR data generally improve classification accuracy (Waske and Braun, 2009; Hütt et al., 2016; Bargiel, 2017). When combined together, SAR and optical data improve crop-type mapping (McNairn et al., 2009; Joshi et al., 2016) and grassland mapping (Hong et al., 2014). However, combined optical-SAR regional rangeland and seeded forage land cover classification studies are lacking.

Recent developments in high (fine) spatial resolution sensors, hyperspectral sensors (e.g., EnMap—German Research Centre for Geosciences/DLR Space Agency), and advanced polarimetric SAR sensors (Sentinel 1—European Space Agency; RADARSAT Constellation Mission—Canadian Space Agency), along with methodological advancements in land cover mapping such as object-based classification (Dingle Robertson and King, 2011; Duro et al., 2012; Goodin et al., 2015) and time-series analysis (Bargiel, 2017), can contribute to improving agricultural land cover classification. However, these data types and processing techniques are associated with large data volumes and/or intensive computational resources that are not readily available for a large-area, national-scale annual land inventory such as that of AAFC, the framework for this study. In this study, this constraint, combined with the potential for seasonal information to discriminate the classes of interest (rangeland, seeded forage, cropland), led to a regional mapping approach using Landsat data, which are generally available for multiple seasons in a given year. In addition, due to known vegetation structural differences among these classes, particularly in midsummer, RADARSAT-2 data were also investigated. The objectives of this study were to 1) determine the type of medium-resolution remotely sensed imagery (optical, SAR, or a combination of both) most useful for accurate mapping of range, forage, and crop land cover classes; 2) evaluate the importance of Landsat data acquisition date within the growing season and derived optical variables (phenology metrics and vegetation indices) for improving classification accuracy; and 3) determine the smallest subset of variables that produces statistically nonsignificant differences in accuracy from the best variable set.
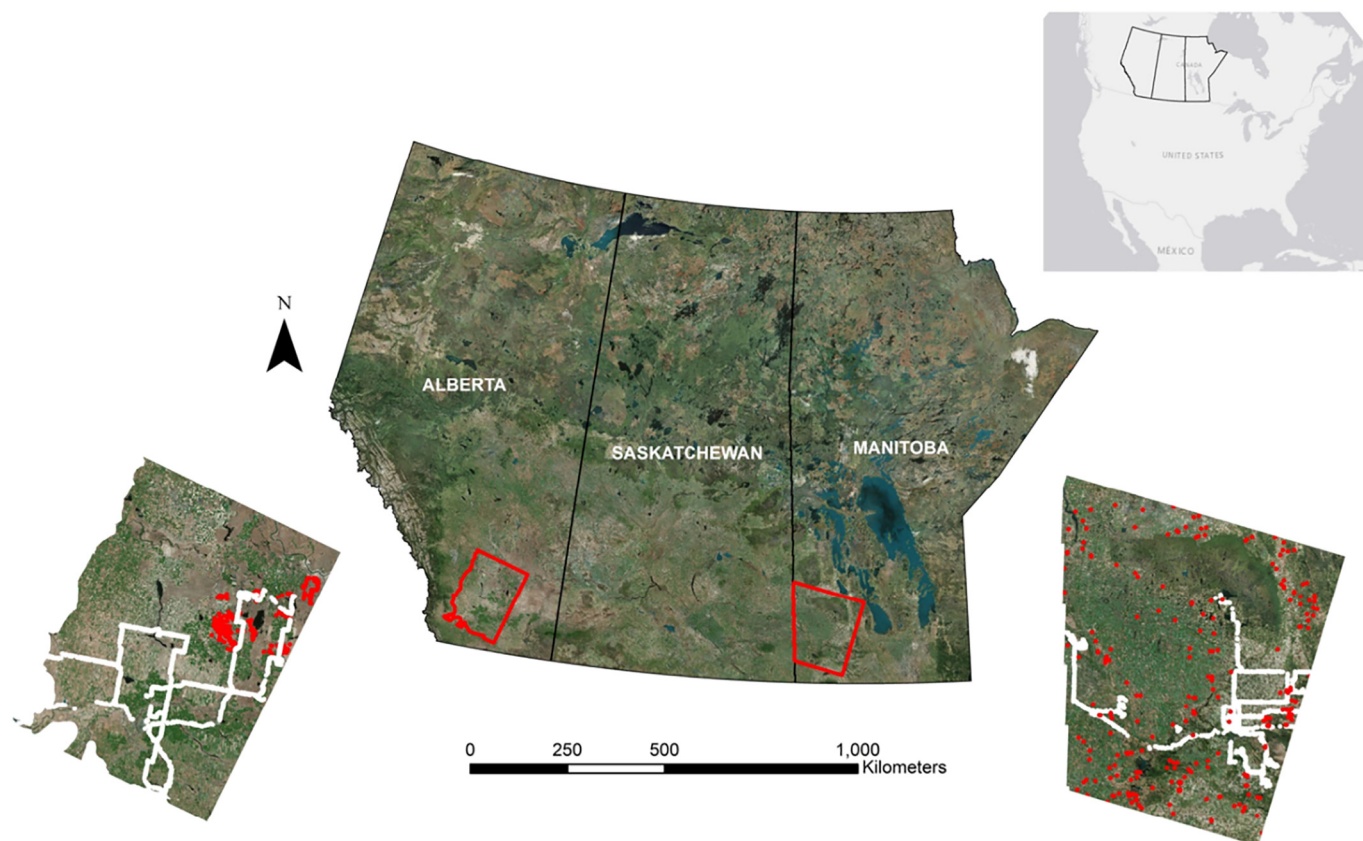

Figure 1. Extent of study areas (red polygons) in Alberta and Manitoba. Routes used for vehicle-based reference information collection are shown in white within the left and right insets. Additional reference data from provincial crop insurance datasets are shown as red data points.

Figure 2. Variability of rangeland class in Alberta study area: A, upland native grassland with marsh lowland in foreground; B, upland native grassland with saline lowland in background; C, native grassland managed as hay (top right) with non-native grass invasion (bottom left). Variability of rangeland class in the Manitoba study area: D, upland native grassland; E, lowland native grassland (foreground) with meadow (middle ground); and F, native tall grass prairie under conservation with shrub encroachment from sides in background. Examples of mature annual cropland class in late summer (20 August, 2013–Winnipeg, Manitoba): G, Late soybean (left of road) and wheat (right of road); and H, flowering canola (left of road) and ripening canola (right of road). (A–C and E − G from Emily Lindsay 2015; D and H, AAFC Crop Inventory 2013.)

Materials and Methods

Study Area

Two geographically distinct areas in the Canadian Prairies were selected to represent the variability of soil, climate, and dominant ecological regions (Fig. 1). The southwestern Alberta study area is 26 650 km², the extent of which corresponded to a Landsat scene that included the Lethbridge, Alberta AAFC research station (WRS Path 041, Row 025). The southwestern Manitoba study area is 31,250 km² and corresponded to a Landsat scene that included the Brandon, Manitoba AAFC research station with the Saskatchewan portion removed as there were no field data collected across the provincial border (WRS Path 033, Row 025). The Manitoba study area receives significantly more precipitation than the Alberta study area (1981 − 2010 climate normal data for Brandon, Manitoba and Lethbridge, Alberta; Environment and Climate Change Canada 2017). It is within the Aspen Parkland Prairie ecoregion, and the corresponding dominant soil type is black chernozem, which is ideally suited to annual crop cultivation (Pennock et al., 2011). In its native state, the Aspen Parkland landscape is characterized by open stands of

Table 1
Remotely sensed data. Landsat 8 images were acquired in spring, summer, and fall seasons when cloud cover was < 10%. RADARSAT-2 imagery was only available for midsummer.

Study area	Sensor	Date of acquisition (doy, 2015)	Season
Manitoba	Landsat 8 OLI	27-May (d147)	Spring
		31-Aug (d243)	Late Summer
		18-Oct (d291)	Fall
	RADARSAT-2	08-Jul (d189)	Mid-Summer
		15-Jul (d196)	Mid-Summer
Alberta	Landsat 8 OLI	19-May (d139)	Spring
		06-Jul (d187)	Mid-Summer
		23-Aug (d235)	Late Summer
	RADARSAT-2	20-Jul (d201)	Mid-Summer
		27-Jul (d208)	Mid-Summer

Table 3
NDVI phenological variables derived from all three dates of Landsat 8 data.

NDVI phenological variable	Description
NDVIMin	Minimum value of NDVI for three dates
NDVIMax	Maximum value of NDVI for three dates
NDVIMean	Mean value of NDVI for three dates
NDVISD	Standard deviation (SD) of NDVI for three dates
NDVICV	Coefficient of Variation (CV) for three dates $CoV = \frac{SD}{Mean}$
NDVIDiff	Difference between NDVI values calculated between all three pairs of two dates

Trembling Aspen *(Populus tremuloides),* and Bur Oak *(Quercus macrocarpa)* with intermittent grasslands on drier sites (Shorthouse, 2010). The Alberta area is mostly dry and moist mixed grassland with larger tracts of undisturbed native rangeland composed of more drought-tolerant plant species adapted to brown and dark brown chernozemic soil types. A large portion of the cultivated cropland and seeded forage in the Alberta study area is irrigated.

Reference Information Collection

Reference information for supervised classification, including dominant species composition of rangeland and seeded forage land cover types, was collected using vehicle surveys (see Fig. 1) in July 2015 during peak grass and annual crop production. The sampling strategy was adjusted to reduce spatial autocorrelation; no more than one site was selected per field, and points were placed no closer than 1 km apart on large continuous tracts of rangeland. A total of 1 581 reference data locations were collected for Alberta, and 1 479 for Manitoba over 1600 kilometers of travel distance. Rangeland and seeded forage land cover types were recorded at the subclass level using class definitions adapted from the Society for Range Management (1998) Glossary of Rangeland definitions. Subclasses of seeded forage included perennial pasture and hay while subclasses of native rangeland included upland native rangeland, meadow, native shrubland, and modified non-native rangeland (i.e., invaded by non-native plants). These subclasses were aggregated to the rangeland and seeded forage classes due to species and spectral similarities within the subclasses, which were expected to hinder their discrimination. Figure 2 shows representative photographs of field conditions for rangeland, seeded forage, and cropland. Supplemental reference data were acquired from provincial crop insurance datasets containing the locations of agricultural land cover types for 2015. Because of the limited remaining rangeland in Manitoba, community pastures were included in this class and accessed to retrieve reference locations when granted permission from land managers and owners.

Remotely Sensed Data Acquisition and Processing

Three Level 1T (terrain corrected) Landsat 8 Operational Land Imager (OLI) scenes were acquired from the US Geologic Survey (USGS)

Landsat data archive for the 2015 growing season for each study area (Table 1). These were the only growing season scenes with < 10% estimated cloud cover (USGS). Midsummer dual polarization (VV and VH) RADARSAT-2 wide-beam mode (W2) imagery were the best available SAR complement to the Landsat 8 imagery. These data had an incidence angle range of 30.6°−39.5° and a pixel size of 25 × 25 m. A total of four scenes (two passes) were acquired to cover the spatial extent of each study area.

Landsat 8 Data Preprocessing and Variables

The Landsat imagery was atmospherically and radiometrically corrected to Top of Atmosphere (TOA) reflectance using the ATCOR-2 algorithm (Richter, 1997). The FMASK algorithm was then applied to remove cloud and cloud shadow (Zhu et al., 2015). The reflectance data for each band were then used to derive several vegetation indices and temporal variables associated with vegetation phenology.

Vegetation indices chosen for this study (Table 2) respond to biophysical properties of grassland vegetation. The common normalized difference vegetation index (NDVI) is representative of photosynthetically active green vegetation (Tucker, 1979). The normalized difference senescent vegetation index (NDSVI) is sensitive to water content and senescent components of vegetation such as litter, crop residue, and senescent grasses (Qi et al., 2002). The soil-adjusted total vegetation index (SATVI) developed from the soil-adjusted vegetation index (SAVI) accounts for the nonphotosynthetically active (yellow) vegetation present in rangeland landscapes and minimizes the influence of soil brightness (Marsett et al., 2006). The wetness component of the Tasseled Cap transformation (Kauth and Thomas, 1976) was used as it correlates well to surface moisture (of soil and vegetation); it was calculated using the updated Landsat 8 coefficients (Baig et al., 2014).

In addition to these four vegetation indices, NDVI phenological variables (Table 3) were derived from the three-date NDVI values for each study area. Rangeland and seeded forage were expected to be green in spring while most crops would not have germinated or would be very short with reflectance due mostly to soil. In addition, rangeland was expected to be green over the whole growing season while seeded forage was expected to show greater temporal variation in greenness due to hay harvesting or more intensive grazing.

Table 2
Vegetation indices used in this study.

Vegetation index	Reference	Equation
NDVI	(Tucker, 1979)	$NDVI = \frac{NIR-R}{NIR+R}$
NDSVI	(Qi et al., 2002)	$NDSVI = \frac{SWIR1-R}{SWIR1+R}$
TCW	(Kauth and Thomas, 1976; Baig et al., 2014)	$TCW = B(0.1511) + G(0.1973) + R(0.3283) + NIR(0.3407) + SWIR1(-0.7117) + SWIR2(-0.4559)$
SATVI	(Marsett et al., 2006)	$SATVI = \frac{SWIR1-R}{SWIR1+R+L}(1+L) - \frac{SWIR2}{2}$

Note: B, G, R, NIR, SWIR1 and SWIR2 are the spectral band reflectance values for Landsat 8. The L value (SATVI) is a constant relating to the slope of the soil line (R-NIR) in a feature-space plot.
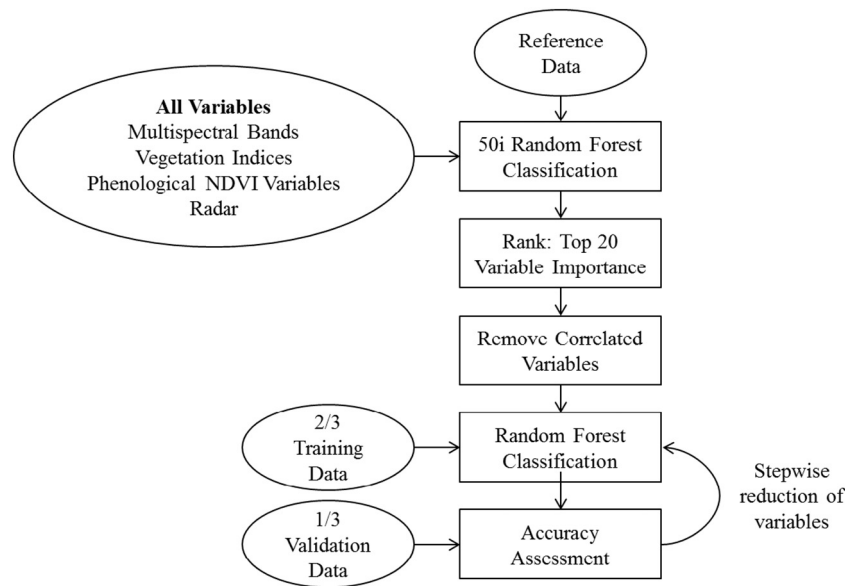
Figure 3. Flowchart of random forest variable reduction method. 50i refers to 50 separate classification iterations performed to analyze variable importance.

RADARSAT-2 Preprocessing and Variables

RADARSAT-2 single-look complex (SLC) VV and VH Wide2 data were ortho-rectified using a Shuttle Radar Topographic Mission (SRTM) DEM (USGS; https://Earthexplorer.usgs.gov), then calibrated to sigma naught (σ^0) backscatter values and filtered using a single-pass gamma MAP filter implemented in a 7 × 7 moving window (Lopes et al., 1990). Images were mosaicked to cover the study areas and resampled from 25 m to 30 m pixel size to match the Landsat 8 images.

Random Forest Classification

Random forest is an ensemble machine learning algorithm for classification and regression (Breiman, 2001). It was implemented here because it performs well on large nonparametric datasets, including multisource Earth observation datasets (Duro et al., 2012; Millard and Richardson, 2013; Dubeau et al., 2017). It can also be used to assess variable importance by estimating the increase in prediction error when each variable is permuted from the rest of the variables (Liaw and Wiener, 2002; Belgiu and Drăguţ, 2016). The random forest classifier

generally outperforms traditional classifiers such as single decision trees and the maximum likelihood classifier and yields comparable levels of accuracy to parameter-intensive machine learning approaches such as Support Vector Machines and Artificial Neural Networks (Waske and Braun, 2009; Deschamps et al., 2012; Duro et al., 2012; Sonobe et al., 2014).

Random forest classification was implemented in R statistics using a script adapted from Millard and Richardson (2015). After assessing error convergence on test classifications, *Ntree,* the number of classification trees to create was set at 1000. *Mtry,* the number of variables to be randomly selected and used to determine the best split at each node (Breiman, 2001), was set at the default value of $\sqrt{p}$ where p is the number of variables used in the classification (Liaw and Wiener, 2002). In addition, before conducting the classification tests, one-third of the reference data were removed and set aside for validation using stratified random sampling based on initial classification using all data and all variables. The number of samples removed for validation was 493 and 527 for the Manitoba and Alberta study areas, respectively. The remaining reference data were used for training, with one-third of those data used in bootstrapped internal (out-of-bag) accuracy assessment of each classification tree. Confusion matrices and associated statistics

Table 4
Accuracy statistics (%) for Landsat 8 multispectral, RADARSAT-2 (RS2), and Landsat 8 (LS8) multispectral + RADARSAT-2 models for the Manitoba study area.

			Overall accuracy	Cropland		Rangeland		Seeded forage		OOB accuracy
				PA	UA	PA	UA	PA	UA	
LS8	Single-date	Spring	84.85	95.82	96.18	54.65	74.60	82.88	71.18	83.40
		Late Summer	85.86	97.72	95.90	59.30	70.83	80.14	75.48	85.48
		Fall	80.61	94.68	88.93	48.84	68.85	73.97	70.13	82.68
	Two-date	Spring & Late Summer	87.88	98.48	96.64	58.14	79.37	86.30	76.83	89.42
		Spring & Fall	88.89	97.34	96.97	67.44	82.86	86.30	78.26	88.69
		Late Summer & Fall	86.26	98.10	95.20	59.30	72.86	80.82	76.62	88.69
	Three-date	Spring, Late Summer & Fall	89.49	98.86	98.86	62.79	78.26	88.36	79.14	90.77
Radar only			68.48	88.21	85.61	38.37	39.76	50.68	52.48	67.84
LS8 + RS2	Single-date	Spring	86.67	95.82	96.55	60.47	80.00	85.62	73.96	86.94
		Late Summer	87.07	97.72	95.90	55.81	76.19	86.30	76.83	87.97
		Fall	84.65	95.82	94.03	60.47	74.29	78.77	73.25	85.06
	Two-date	Spring & Late Summer	88.69	97.72	98.09	61.63	80.30	88.36	77.25	90.26
		Spring & Fall	88.69	97.34	97.64	62.79	83.08	88.36	77.25	90.25
		Late Summer & Fall	89.09	99.24	96.31	63.95	80.88	85.62	80.13	90.87
	Three-date	Spring, Late Summer & Fall	89.49	98.86	98.48	63.95	78.57	87.67	79.50	91.70

PA indicates producer's accuracy; UA is user's accuracy (both PA and UA are used in independent validation); OOB, random forest out-of-bag sample.

Table 5
Accuracy statistics (%) for Landsat 8 multispectral, RADARSAT-2, and Landsat 8 multispectral + RADARSAT-2 models for the Alberta study area ($n = 527$).

			Overall accuracy	Cropland		Rangeland		Seeded forage		OOB accuracy
				PA	UA	PA	UA	PA	UA	
LS8	*Single-date*	Spring	88.80	90.68	92.53	90.97	93.57	81.82	75.63	89.12
		Mid Summer	86.40	93.50	86.47	88.89	94.12	67.27	75.51	83.97
		Late Summer	88.00	96.34	92.58	83.33	89.55	75.45	75.45	87.89
	Two-date	Spring & Mid Summer	90.60	95.12	93.98	89.58	94.16	81.82	81.82	91.00
		Spring & Late Summer	91.20	97.56	94.12	88.19	91.37	80.91	80.91	91.89
		Mid Summer & Late Summer	89.80	95.53	92.16	88.19	94.07	79.09	79.09	87.68
	Three-date	Spring, Mid Summer & Late Summer	92.80	96.75	95.58	90.97	95.62	86.36	83.33	92.53
Radar only			75.80	87.80	76.60	84.72	87.77	37.27	51.90	74.62
LS8 + RS2	*Single-date*	Spring	88.60	91.46	93.36	90.28	93.53	80.00	73.33	91.19
		Mid Summer	88.00	92.28	88.33	90.97	95.62	74.55	77.36	85.47
		Late Summer	88.20	95.12	92.86	85.42	92.48	76.36	73.04	88.19
	Two-date	Spring & Mid Summer	91.40	96.34	92.58	90.97	96.32	80.91	82.41	91.93
		Spring & Late Summer	91.80	97.15	94.84	89.58	94.16	82.73	81.98	93.10
		Mid Summer & Late Summer	90.00	95.93	92.91	87.50	94.03	80.00	78.57	89.54
	Three-date	Spring, Mid Summer & Late Summer	92.20	96.75	94.82	90.97	95.62	83.64	82.14	92.87

PA indicates producer's accuracy; UA is user's accuracy (both PA and UA are used in independent validation); OOB, random forest out-of-bag sample.

Table 6
Accuracy statistics (%) for combinations of Landsat 8 three-date multispectral (MS), vegetation index (VI), and phenological NDVI (PhenNDVI) variables for the Manitoba and Alberta study areas.

		Overall accuracy	Cropland		Rangeland		Seeded forage		OOB accuracy
3-Date LS8 variables			PA	UA	PA	UA	PA	UA	
Manitoba	MS	89.49	98.86	98.86	62.79	78.26	88.36	79.14	90.77
	VI	81.82	98.86	92.86	47.67	58.57	71.23	71.72	82.78
	PhenNDVI	81.82	93.92	91.82	52.33	66.18	77.40	71.52	81.74
	MS + VI	89.29	98.86	98.86	62.79	77.14	87.67	79.01	90.98
	VI + PhenNDVI	87.07	98.48	96.64	56.98	75.38	84.25	75.93	88.91
	MS + PhenNDVI	88.89	98.48	98.48	60.47	78.79	88.36	77.71	90.46
	MS + VI + PhenNDVI	88.69	98.86	98.11	60.47	78.79	86.99	77.44	89.94
Alberta	MS	92.80	96.75	95.58	90.97	95.62	86.36	83.33	92.53
	VI	93.60	99.19	94.57	91.67	95.65	83.64	88.46	91.90
	PhenNDVI	92.60	95.12	96.30	94.44	90.67	84.55	86.92	90.38
	MS + VI	92.60	97.97	95.26	89.58	95.56	84.55	83.04	92.87
	VI + PhenNDVI	94.40	98.78	96.05	91.67	96.35	88.18	88.18	93.40
	MS + PhenNDVI	91.80	96.75	90.28	82.73	95.20	94.20	81.25	92.45
	MS + VI + PhenNDVI	93.60	97.97	96.40	90.97	95.62	87.27	84.96	92.47

PA indicates producer's accuracy; UA is user's accuracy (both PA and UA are used in independent validation); OOB, random forest out-of-bag sample.

were generated, and pairwise overall model performance was assessed using McNemar's test (McNemar, 1947; Foody, 2004; Dingle Robertson and King, 2011). McNemar's test is based on a 2×2 contingency table representing the cross-tabulation of the correct and incorrect class distributions for each map. The contingency table cells are f_{11}, the number of samples correct in both maps; f_{22}, the number of samples incorrect in both maps; f_{12}, the number of correct pixels in one map that are incorrect in the other map; and f_{21}, the opposite of f_{12}. The square of $[Z = (f_{12}-f_{21})/(f_{12} + f_{21})^2]$ follows a chi-squared distribution. Pairs of classifications were tested to determine if they were significantly different ($P < 0.05$). More detail on this test is given in the references.

Classifications were performed on optical and SAR variables separately and together to assess the relative contributions of each image type. Classifications were also performed using 1) all possible single-date, two-date, and three-date Landsat 8 bands; 2) as for 1) using the vegetation indices; and 3) the derived phenological variables to assess the importance of multitemporal data across the growing season. From these tests, the variable set that produced the best overall accuracy was determined.

Table 7
Manitoba variable reduction results.

Number of variables	Overall accuracy	Cropland		Rangeland		Seeded forage		OOB error
		PA	UA	PA	UA	PA	UA	
40	88.48	98.48	97.37	60.47	80.00	86.99	77.44	90.66
8	87.80	98.48	98.48	62.79	76.06	86.30	78.26	90.88
7	88.48	98.48	98.48	61.63	74.65	86.30	78.26	90.77
6	88.28	97.72	98.09	62.79	77.14	86.30	77.30	90.66
5	87.20	97.34	98.08	61.63	76.81	86.99	76.97	90.46
4	86.40	96.58	96.58	62.79	77.14	84.93	76.54	89.21
3*	85.86	96.20	96.56	59.30	70.83	82.88	75.16	87.66
2*	80.80	95.82	94.74	60.47	59.77	68.49	70.42	80.39

PA indicates producer's accuracy; UA is user's accuracy (both PA and UA are used in independent validation); OOB, random forest out-of-bag sample.
 * Significantly different ($P \leq 0.05$) than the classification using all 40 variables.

Table 8
Alberta variable reduction results.

Number of variables	Overall accuracy	Cropland		Rangeland		Seeded forage		OOB error
		PA	UA	PA	UA	PA	UA	
40	94.00	97.97	96.02	91.67	96.35	88.18	86.61	93.73
8	93.20	97.56	96.39	89.58	95.56	88.18	83.62	92.70
7	93.60	97.56	96.00	90.28	96.30	89.09	85.22	92.30
6	93.20	97.15	95.60	89.58	95.56	89.09	85.22	91.97
5	92.80	96.34	95.56	89.58	94.85	89.09	84.48	91.34
4*	91.60	96.34	94.80	87.50	92.65	86.36	83.33	90.19
3*	88.80	94.31	93.93	85.42	85.42	80.91	81.65	87.45
2*	80.40	87.80	92.31	77.08	68.10	68.18	72.82	79.65

PA indicates producer's accuracy; UA is user's accuracy (both PA and UA are used in independent validation); OOB, random forest out-of-bag sample.
 * Significantly different (P ≤ 0.05) than the classification using all 40 variables.

Table 9
Spearman rank correlation (ρ) for the eight most important and uncorrelated random forest input variables, Manitoba study area.

	1	2	3	4	5	6	7	8
1. RS2 VH	1.00							
2. SWIR2 (d147)	0.58	1.00						
3. NDVI (d291)	−0.44	−0.53	1.00					
4. NIR (d147)	−0.53	−0.62	0.58	1.00				
5. Red (d243)	0.20	0.41	−0.34	−0.39	1.00			
6. Red (d291)	0.32	0.50	−0.48	−0.28	0.30	1.00		
7. NDVI CV	0.13	0.33	−0.52	0.19	0.72	0.20	1.00	
8. SATVI (d291)	−0.49	−0.66	0.72	0.47	−0.38	−0.75	−0.36	1.00

NDVI, normalized difference vegetation index; SATVI, soil-adjusted total vegetation index; NDVICV, coefficient of variation of NDVI; Red, NIR and SWIR2 are Landsat 8 spectral band reflectance; RS2 VH is RADARSAT-2 VH backscatter. Day of year is noted in brackets.

Random Forest Variable Importance Analysis and Determination of Optimal Variable Subset

Random forest classification was used to assess variable importance (objective 2), to determine the impact of strategic removal of less important variables on classification accuracy. From this, the optimal subset of variables that achieved overall classification accuracy not statistically lower than that of the best variable set (objective 3) was determined in order to improve computational efficiency. Fifty separate classifications were conducted for each study area using all 40 Landsat 8 variables (multispectral bands, vegetation indices, NDVI phenological variables) and RADARSAT-2 backscatter variables (Fig. 3). All reference data were used in model training. The mean decrease in accuracy variable importance measure was used to rank the importance of each variable in the 50 classifications (Breiman, 2001). It is evaluated by the difference in prediction accuracy before and after permuting the predictor variable (Strobl et al., 2008). The top 20 variables were determined by ranking the 40 variables on the basis of this metric in each classification and adding the ranks over all 50 classifications. Between-variable Spearman rank correlation (ρ) within this top-20 set was then reduced by removing the variable of lesser importance from any highly correlated (ρ > 0.80) variable pair. This process helped increase model efficiency and reduce the chance of model overfitting (Millard and Richardson, 2015). Random forest was then implemented on the set of most important uncorrelated variables. Additional classifications were performed using one less variable each time (i.e., the variable of lowest importance was dropped in a stepwise fashion until only two variables remained). The performance of each of these models was assessed using the one-third independent validation set. McNemar's test was used to determine the minimum number of variables that could achieve statistically similar results to the best classification.

Results

In general, when comparing pairs of classifications using the one-third reference data set aside for independent validation, McNemar's test was significant (P ≤ 0.05) for overall accuracy differences of approximately 1.8% or more. Therefore, in Tables 4-6, 9, and 10, any pair of classifications with overall accuracy differing by >1.8% were considered to be significantly different. Also, in Tables 4-6, out-of-bag accuracy was found to be <± 2.5% for all classifications. This small difference indicates that the models were not overfit; such overfitting typically would result in much higher out-of-bag accuracy than independent validation accuracy.

Table 10
Spearman rank correlation (ρ) for the eight most important and uncorrelated random forest input variables, Alberta study area.

	1	2	3	4	5	6	7	8
1. NDVI Min	1.00							
2. NDVI CV	−0.67	1.00						
3. NIR (d139)	0.49	−0.28	1.00					
4. SWIR2 (d139)	−0.58	0.67	−0.11	1.00				
5. TCW (d139)	0.60	−0.65	0.22	−0.79	1.00			
6. NDSVI (d235)	0.42	−0.64	−0.11	−0.58	−0.75	1.00		
7. RS2 VV	−0.29	0.45	0.24	0.53	0.75	−0.69	1.00	
8. Red (d235)	−0.33	0.63	−0.01	0.33	−0.30	−0.34	0.18	1.00

TCW, Tasseled Cap Wetness; NDSVI, normalized difference senescent vegetation index; NDVIMin, minimum value of NDVI for three dates; NDVICV, coefficient of variation of NDVI; Red, NIR, and SWIR2 are spectral band reflectance; RS-2 VV is RADARSAT-2 VV backscatter. Day of year is noted in brackets.
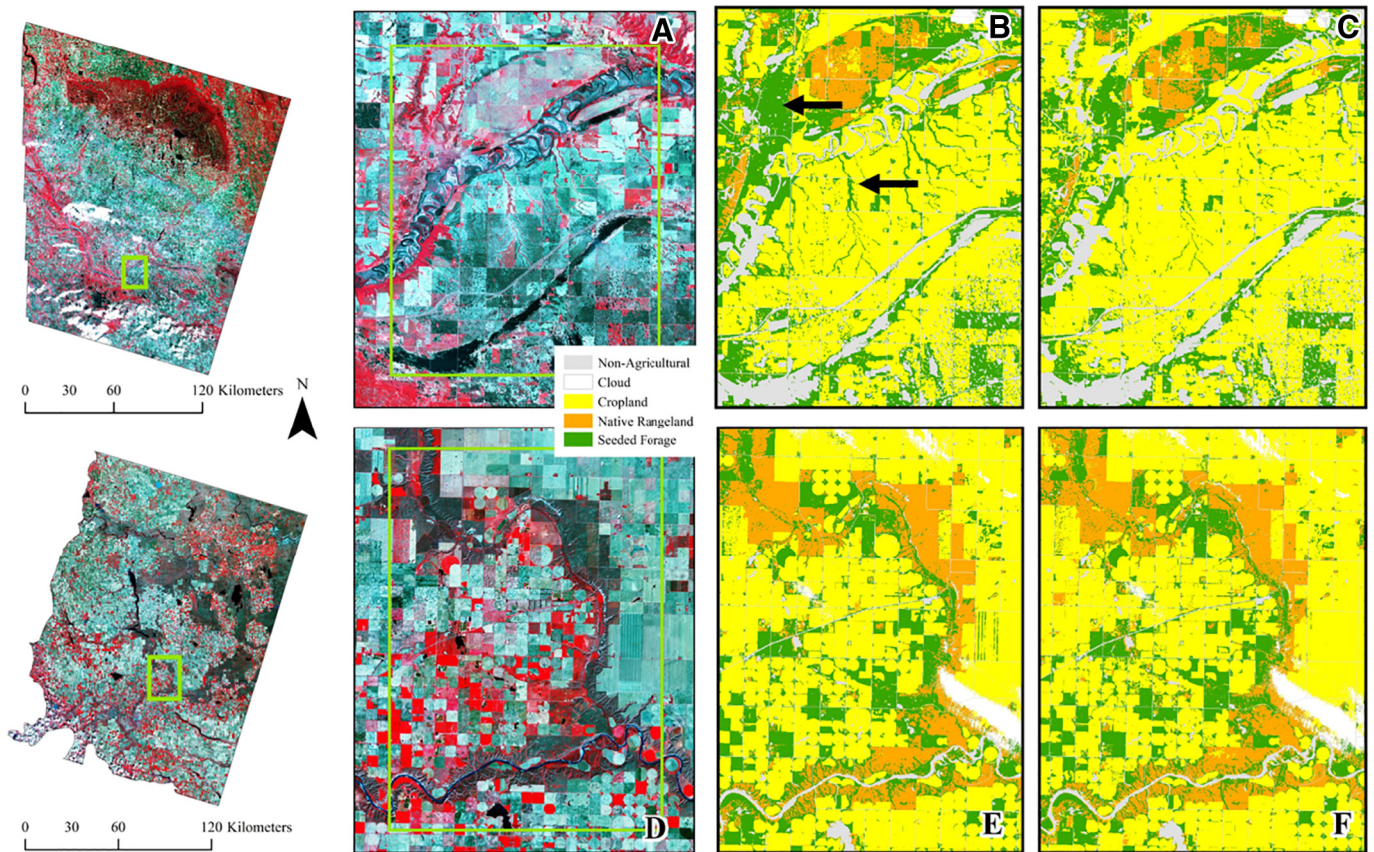
Figure 4. Random forest classification for the Manitoba study area: **A,** Landsat 8 spring false-color composite of the inset in the upper left image; **B,** classification using all 40 Landsat 8 and RADARSAT-2 variables; and **C,** classification using top 4 variables. Random forest classification for the Alberta study area: **D,** Landsat 8 spring false-color composite of the inset in the lower left image; **E,** classification using all 40 Landsat 8 and RADARSAT-2 variables; and **F,** classification using top 5 variables.

Classification Accuracy for Single-, Two-, and Three-Date Landsat 8 Multispectral Data

There were no significant differences in overall classification accuracy when Landsat 8 multispectral reflectance data were used as input versus vegetation indices. Therefore, results presented in Tables 4 and 5 are for Landsat 8 multispectral data, which require less processing. Of the single-season results, overall accuracy was highest for spring (Alberta study area) or late summer (Manitoba study area), but in both cases accuracies for these two seasons were not significantly different from the results for the other seasons. Cropland was generally better classified using late summer data. However, rangeland and seeded forage were best classified using spring data (Alberta) and spring or late summer data (Manitoba).

Three-date Landsat 8 multispectral data performed the best and were significantly better than all two-date classifications for both study areas, with the exception of the Manitoba study area spring-fall data, which produced an overall accuracy only 0.6% less than that for the three-date data. It is evident from Tables 4 and 5 that if only two-season data can be acquired, spring and fall or spring and late summer are best. Spring optical data are important to distinguish rangeland and seeded forage from cropland.

Classification Accuracy for Landsat 8 Multitemporal Variable Groups

Results presented in Table 6 are the random forest classifier performance for the three-date optical variable groups alone and in combination. The three variables groups in order of increasing preprocessing effort were the six Landsat 8 multispectral bands, the four vegetation index variables, and then the eight phenological NDVI variables derived from the three NDVI image dates. The Manitoba results in Table 6

indicate that the three-date vegetation index and phenological NDVI classifications each had significantly lower overall accuracy than the three-date multispectral variable classification (89.49%). However, the corresponding Alberta classifications for these three data types did not differ significantly in overall accuracy.

Classification Accuracy for Midsummer RADARSAT-2 and [RADARSAT-2 + Landsat 8] Data

Classification using only RADARSAT-2 VV and VH backscatter did not perform well for the Manitoba study area (68.48% overall accuracy) but was better for the Alberta study area (75.80% overall accuracy) (see Tables 4 and 5). Confusion was high between seeded forage and rangeland (Manitoba) and between cropland and seeded forage (Alberta). In the Alberta study area, rangeland was well classified using the RADARSAT-2 data relative to cropland and seeded forage classes (84.72% Producer's Accuracy, 87.77% User's Accuracy); this may be because native rangeland vegetation is generally shorter in height and drier than seeded forage and crops in midsummer, therefore producing a distinct backscatter response. In Alberta, the abundance of irrigated cropland and seeded forage creates a more distinctive difference in aboveground biomass, and thus a greater separability of backscatter values when compared with drier sites of native rangeland.

Combining RADARSAT-2 and Landsat 8 data produced overall accuracies that were mostly higher than for the Landsat 8 variables alone (see Tables 4 and 5); however, not all increases were significant ($P <$ 0.05). Increases were most pronounced ($1-4\%$) for the Manitoba study area (see Table 4) when RADARSAT-2 data were included with single-date spring or fall Landsat 8 data. RADARSAT-2 data added to two-date Landsat 8 late summer and fall data also produced significant improvements. However, adding RADARSAT-2 data to two-date Landsat

8 data where one date included spring, or to three-date Landsat 8 data, did not produce significant improvements. With respect to individual class accuracy, for the Manitoba area, adding RADARSAT to Landsat 8 data improved the accuracy of rangeland the most, particularly when it was added to fall Landsat (Producer's Accuracy increase = 11.6%; User's Accuracy increase = 5.4%). Adding it to two-date Landsat 8 data improved rangeland Producer's Accuracy and User's Accuracy in five of six cases but by smaller amounts, while adding it to three-date Landsat 8 data produced accuracy increases of < 1.2%. Seeded forage showed a similar pattern of accuracy increases when RADARSAT-2 data were added to single- and two-date Landsat 8 data but with slightly lower increases than for rangeland. Cropland did not show appreciable increases when the two data types were combined. These results show that for the Manitoba study area, if only one or two of the spring, late summer, and fall Landsat image dates are available, adding RADARSAT-2 backscatter is beneficial, whereas if Landsat 8 data can be acquired in all three seasons, there is no point in adding RADARSAT-2 data to the classification.

Overall accuracy did not increase significantly when RADARSAT-2 data were added to any combination of Landsat 8 data for the Alberta study area (see Table 5). Rangeland and seeded forage again increased in accuracy when RADARSAT-2 data were added to single- or two-date Landsat 8 data, but the increases were mostly in the 1−3% range and, in a few cases, there was no increase or a decrease in Producer's Accuracy or User's Accuracy.

Variable Importance Analysis and Determining of Optimal Variable Subset

A single iteration of the classification using all 40 Landsat 8 and midsummer RADARSAT-2 variables produced an overall classification accuracy of 88.48% for the Manitoba study area (Table 7) and 94.00% for the Alberta study area (Table 8). For the latter, overall accuracy using all 40 variables was significantly (1.8%) better than using three-date Landsat 8 multispectral and midsummer RADARSAT-2 data (see Table 5). However, for the Manitoba study area overall accuracy using 40 variables was 1% lower than the three-date Landsat 8 multispectral + RADARSAT-2 classification (see Table 4), indicating that the 40 variable classification may have been overfit due to variable correlation.

In the variable importance analysis, the top 20 variables were selected and reduced further to a subset of eight that were not highly correlated ($\rho < 0.80$; Tables 9 and 10). Iterative classifications conducted with one less variable each time (i.e., by dropping the least important variable) showed that overall accuracies were not statistically different from the 40-variable classification up to a minimum of four (Manitoba, see Table 7) and five (Alberta, see Table 8) variables. In the Manitoba model, the most important variable was RADARSAT-2 VH backscatter (highly correlated [$\rho = 0.86$] with VV backscatter), followed by three optical variables: Spring SWIR2 reflectance, Fall NDVI, and Spring NIR reflectance. In the Alberta model the most important variable was minimum NDVI derived from the three available Landsat imaging dates. It was highly correlated with spring NDVI ($\rho = 0.83$) because only three dates of Landsat imagery were acquired. The other four variables by decreasing importance were the coefficient of variation of NDVI over the three seasons (NDVICV), Spring NIR reflectance, Spring SWIR2 reflectance, and Spring Tasseled Cap Wetness (TCW). Spring TCW was highly important in Alberta, while spring NIR and SWIR2, as well as the coefficient of variation of NDVI, were important variables for both study areas.

Figure 4 provides a visual comparison of the maps produced using all 40 variables, and the maximally reduced variable set for Manitoba (4 variables) and Alberta (5 variables). The 40 variable and reduced variable maps appear to be similar, but the 40 variable maps have less noise and more connectivity between classes. Some visible differences are also evident. For example, at the *upper arrow* in (**B**), the area classified solidly as seeded forage (green) is classified as seeded forage and cropland in (**C**). The latter is an error as this area was seeded forage.

At the *lower arrow,* green lines are visible in (**B**) that are not present or faintly present in (**C**). These lines follow lowland riparian areas adjacent to agricultural land. They are not seeded forage as classified in the 40-variable map, and they are also not crop as classified in the 4-variable map. Given that only three classes were used, pixels such as these were wrongly classified in both models. In future work, hydrology data should be used to mask or create a buffer of such features.

Discussion

Interpretation of Main Findings

This study found that multiseason Landsat 8 imagery, acquired during key phenological stages in the growing season, provides significantly better classification accuracy of rangeland, seeded forage, and cropland than a single-date image. This concurs with other studies that have used the temporal differences in spring green-up between vegetation types for land cover classification (Li et al., 2015; Gómez et al., 2016) and grassland mapping (Wang, Hunt, et al., 2013; McInnes et al., 2015). A primary reason for improved accuracy using temporal information is that the rate of spring green-up is known to be slower for native versus non-native grasses in mixed-grass environments (McInnes et al., 2015). For sensors such as Landsat with relatively low temporal resolution, if only a single image can be acquired in a growing season (e.g., due to cloud cover), this study generally found no significant differences in overall accuracy between seasons. However, spring imagery better distinguished native rangeland from seeded forage, as well as cropland from perennial vegetation, due to added bare soil reflectance effects in spring-planted crop fields. Indeed, for such classifications the timeliness of optical imagery acquisition has been shown to be more important than the spectral resolution of the optical data (Ali et al., 2016).

The vegetation index and phenological NDVI variable groups did not perform as well as simple multispectral band reflectance, although differences in overall accuracy were often not statistically significant. However, variable importance analysis to derive optimal variable subsets revealed that individual variables from these two groups contributed strongly to classifications. For example, the coefficient of variation of NDVI is sensitive to the phenological differences in native rangeland and seeded forage types, which are most pronounced early and later in the growing season (Tieszen et al., 1997). Thus, these temporal variables can be useful when combined with, and not correlated with, multispectral band reflectance. Palchowdhuri et al. (2018) found similar results for crop type mapping in the United Kingdom using three vegetation indices derived from multitemporal Worldview-3 and Sentinel-2 imagery. Jia et al. (2014) found that temporal NDVI variables (minimum, maximum, mean, and standard deviation) derived from fused Landsat and MODIS data performed better than multispectral bands for regional classification of vegetation types in China. Additional exploration into functionally based vegetation indices may yield better results in grassland environments (Yang et al., 2017).

Midsummer RADARSAT-2 backscatter did not perform well on its own but significantly increased overall accuracy when combined with single- and two-date Landsat 8 multispectral bands for the Manitoba study site. In the variable importance analysis, VH backscatter was ranked first in the Manitoba study area. SAR provides unique information on the structural and dielectric properties of vegetation and soil that contributed to improved discrimination of rangeland from seeded forage and cropland. The use of dual-polarized (VV and HV) C-Band SAR for agricultural land cover classification is well supported by the literature (McNairn and Shang, 2016; Guo et al., 2018). SAR provides the best accuracy for distinguishing crop types at peak biomass (McNairn et al., 2009), and the use of multitemporal and multipolarization SAR data improves crop classification accuracy (Salehi et al., 2017). Consequently, such SAR data should be added to optical data in this ecoregion, particularly when three-season optical data cannot be acquired (e.g.,

due to cloud cover). In the Alberta study area, addition of SAR to single- or multi-date multispectral data did not result in significant overall accuracy improvements. This may be because the Alberta area is drier and rangeland is not as green as seeded forage throughout the growing season resulting in spectral reflectance differences between these two classes that can be well classified with optical data alone. In the Manitoba area, SAR backscatter values were probably sensitive to the greater variation in soil and vegetation water content (Wang, Ge, and Li, 2013).

Recently, the temporal and spatial resolution of optical and SAR satellite platforms has been improved by constellation missions such as the European Space Agency's Sentinel 1A/B (6-day revisit) and 2 A/B (5-day revisit) and daily revisit from Planet Labs' RapidEye constellation, as well as Digital Globe's WorldView constellation. With the development of new SAR sensors providing increased temporal frequency and polarimetric capabilities, further research is needed on the importance of acquisition dates, incidence angles, beam modes, and polarimetric characteristics in regional rangeland mapping applications (Buckley and Smith, 2016) and on the use of multiple wavelengths including X-band (Metz et al., 2014), L-band (Barrett et al., 2014).

The use of random forest classification in this study was supported by past studies, which found it to be well suited to multisource Earth observation data with a limited possibility of overfitting (Millard and Richardson, 2013; Behnamian et al., 2017; Zhang et al., 2017; Dubeau et al., 2017). In addition to being a popular algorithm for land cover classification, random forest is an improvement on the single Decision Tree classifier that had been in use for AAFC's annual crop inventory (Fisette et al., 2014; Davidson et al., 2017). The method of variable importance analysis and variable reduction implemented using random forest was particularly valuable, showing that a subset of $4 - 5$ variables can achieve statistically similar overall accuracy to a set of 40 variables. These results are consistent with White et al. (2017), who used random forest variable importance measures to reduce the number of variables for classification of a peatland system.

The primary limitation of this study that needs continued attention is the availability and acquisition of appropriate reference and Earth observation data. In the Canadian Prairies, a single crop (seeded forage and annual crops) typically covers a maximum of ~0.65 km^2 (or a quarter section) and areas of rangeland are often larger. Ground-based visual inventory of land cover has been the most common approach (Fisette et al., 2014). In this study, to achieve adequate training and validation sample sizes for each class and to minimize spatial autocorrelation between observations, many days of continuous driving were required. Performance of ground-based visual identification of rangeland and forage land cover type is also limited by the expertise of the user (Ali et al., 2016). In particular, distinguishing native rangeland and seeded forage types was difficult in some areas of Manitoba where greater seasonal precipitation results in similar height and greenness for these classes. This may be the cause of the lower producer's accuracy for rangeland in the Landsat classifications and for seeded forage in the SAR classification. In future work, other forms of reference data collection, including potentially the use of UAV (drone)-based photos, should be implemented.

Implications

Spatial and temporal information on Prairie vegetation cover types is critical for understanding the extent and dynamics of ecosystems managed for natural values or agricultural production. It can contribute significantly to development of policy for protection of areas of native rangeland or seminatural perennial land cover that may be threatened by land conversion and ecological degradation. This study demonstrated that rangeland, seeded forage, and cropland can be accurately mapped using three-season Landsat data or two-season Landsat data in combination with single-season SAR data. High accuracies for two areas in Manitoba and Alberta, each about $26\,000 - 31\,000$ km^2, were achieved using these data. However, throughout the Prairies there is

significant regional variability in management and vegetation composition of rangeland and seeded forage. Further testing is needed in other areas to determine the capability for spatial extension of the method. In particular, for operational mapping over large areas such as the AAFC agriculture inventory, data volumes and processing are a primary concern. Higher frequency data will be required to capture phenological differences between these classes across the full extent of the Prairies. With the coming RADARSAT Constellation and other data sources, high temporal frequency polarimetric SAR data will play a more significant role. As a consequence, derivation of optimal variable subsets through techniques such as random forest-based variable importance analysis, as was conducted here, will be increasingly useful to manage data processing and computational efficiency.

References

Ali, I., Cawkwell, F., Dwyer, E., Barrett, B., Green, S., 2016. Satellite remote sensing of grasslands: from observation to management. Journal of Plant Ecology 9 (6), 649–671.

Baig, M.H.A., Zhang, L., Shuai, T., Tong, Q., 2014. Derivation of a tasselled cap transformation based on Landsat 8 at-satellite reflectance. Remote Sensing Letters 5 (5), 423–431.

Bailey, A.W., Bailey, P.G., 1994. The traditions of our ancestors influence rangeland management. Rangelands Archives 16 (1), 29–32.

Bargiel, D., 2017. A new method for crop classification combining time series of radar images and crop phenology information. Remote Sensing of Environment 198 (Supplement C), 369–383. https://doi.org/10.1016/j.rse.2017.06.022.

Barrett, B., Nitze, I., Green, S., Cawkwell, F., 2014. Assessment of multi-temporal, multi-sensor radar and ancillary spatial data for grasslands monitoring in Ireland using machine learning approaches. Remote Sensing of Environment 152, 109–124.

Behnamian, A., Millard, K., Banks, S.N., White, L., Richardson, M., Pasher, J., 2017. A systematic approach for variable selection with random forests: achieving stable variable importance values. IEEE Geoscience and Remote Sensing Letters 14 (11), 1988–1992.

Belgiu, M., Drăguţ, L., 2016. Random forest in remote sensing: a review of applications and future directions. ISPRS Journal of Photogrammetry and Remote Sensing 114, 24–31.

Breiman, L., 2001. Random Forests. Machine Learning 45 (1), 5–32.

Buckley, J.R., Smith, A.M., 2016. Optimizing remote sensing of native grasslands for monitoring and change detection. 2016 IEEE International Geoscience and Remote Sensing Symposium (IGARSS), pp. 159–161.

Davidson, A.M., Fisette, T., McNairn, H., Daneshfar, B., 2017. Detailed crop mapping using remote sensing data (Crop Data Layers). In: Delince, J. (Ed.), Handbook on remote sensing for agricultural statistics (Chapter 4). Handbook of the global strategy to improve agricultural and rural statistics (GradarS), pp. 91–117.

Deschamps, B., McNairn, H., Shang, J., Jiao, X., 2012. Towards operational radar-only crop type classification: comparison of a traditional decision tree with a random forest classifier. Canadian Journal of Remote Sensing 38 (1), 60–68.

Dingle Robertson, L., King, D.J., 2011. Comparison of pixel- and object-based classification in land cover change mapping. International Journal of Remote Sensing 32 (6), 1505–1529.

DiTomaso, J.M., 2000. Invasive weeds in rangelands: species, impacts, and management. Weed Science 48 (2), 255–265.

Dubeau, P., King, D., Unbushe, D., Rebelo, L.-M., 2017. Mapping the Dabus Wetlands, Ethiopia, using random forest classification of Landsat, Producer's AccuracyLradar and Topographic Data. Remote Sensing 9 (12), 1056.

Duro, D.C., Franklin, S.E., Dubé, M.G., 2012. Multi-scale object-based image analysis and feature selection of multi-sensor earth observation imagery using random forests. International Journal of Remote Sensing 33 (14), 4502–4526.

Ecological Stratification Working Group, 1995. A National Ecological Framework for Canada (Report and National Map at 1:7 500 000 scale). 125. Agriculture and Agri-Food Canada, Research Branch, Centre for Land and Biological Resources Research and Environment Canada, Ottawa, ON.

Fisette, T., Davidson, A.M., Daneshfar, B., Rollin, P., Aly, Z., Campbell, L., 2014. Annual Space-Based Crop Inventory for Canada: 2009-2014 (pp. 5095–5098). Presented at the 2014 IEEE International Geoscience and Remote Sensing Symposium, Quebec City, QC. https://doi.org/10.1109/IGARSS.2014.6947643

Foody, G.M., 2004. Thematic map comparison: evaluating the statistical significance of differences in classification accuracy. Photogrammetric Engineering & Remote Sensing 70 (5), 627–633.

Fox, T.A., Barchyn, T.E., Hugenholtz, C.H., 2012. Successes of soil conservation in the Canadian Prairies highlighted by a historical decline in blowing dust. Environmental Research Letters 7 (1), 014008.

Fuhlendo Random Forest, S.D., Engle, D.M., Elmore, R.D., Limb, R.F., Bidwell, T.G., 2012. Conservation of pattern and process: developing an alternative paradigm of rangeland management. Rangeland Ecology & Management 65 (6), 579–589.

Gómez, C., White, J.C., Wulder, M.A., 2016. Optical remotely sensed time series data for land cover classification: a review. ISPRS Journal of Photogrammetry and Remote Sensing 116, 55–72.

Goodin, D.G., Anibas, K.L., Bezymennyi, M., 2015. Mapping land cover and land use from object-based classification: an example from a complex agricultural landscape. International Journal of Remote Sensing 36 (18), 4702–4723.

Guo, J., Wei, P.L., Liu, J., Jin, B., Su, B.F., Zhou, Z.S., 2018. Crop classification based on differential characteristics of h/α scattering parameters for multitemporal quad- and dual-polarization SAR images. IEEE Transactions on Geoscience and Remote Sensing PP (99), 1–13.

Hall-Beyer, M., 2012. Patterns in the yearly trajectory of standard deviation of NDVI over 25 years for forest, grasslands and croplands across ecological gradients in Alberta, Canada. International Journal of Remote Sensing 33 (9), 2725–2746.

Hong, G., Zhang, A., Zhou, F., Brisco, B., 2014. Integration of optical and synthetic aperture radar (radar) images to differentiate grassland and alfalfa in Prairie area. International Journal of Applied Earth Observation and Geoinformation 28 (Suppl C), 12–19.

Hütt, C., Koppe, W., Miao, Y., Bareth, G., 2016. Best accuracy land use/land cover (LULC) Classification to derive crop types using multitemporal, multisensor, and multi-polarization radar satellite images. Remote Sensing 8 (8), 684.

Jansen, V.S., Kolden, C.A., Taylor, R.V., Newingham, B.A., 2016. Quantifying livestock effects on bunchgrass vegetation with Landsat ETM + data across a single growing season. International Journal of Remote Sensing 37 (1), 150–175.

Jia, K., Liang, S., Zhang, N., Wei, X., Gu, X., Zhao, X., Yao, X., Xie, X., 2014. Land cover classification of finer resolution remote sensing data integrating temporal features from time series coarser resolution data. ISPRS Journal of Photogrammetry and Remote Sensing 93, 49–55.

Joshi, N., Baumann, M., Ehammer, A., Fensholt, R., Grogan, K., Hostert, P., Jepsen, M., Kuemmerle, T., Meyfroidt, P., Mitchard, E., Reiche, J., Casey, R., Waske, B., 2016. A review of the application of optical and radar remote sensing data fusion to land use mapping and monitoring. Remote Sensing 8 (1), 70.

Kauth, R.J., Thomas, G.S., 1976. The tasseled Cap – A Graphic Description of the Spectral-Temporal Development of Agricultural Crops as Seen by LANDSAT. Proceedings of the Symposium on Machine Processing of Remotely Sensed Data. Purdue University of West Lafayette, Indiana pp. 4B-41 to 4B-51.

Li, Q., Wang, C., Zhang, B., Lu, L., 2015. Object-based crop classification with Landsat-MODIS enhanced time-series data. Remote Sensing 7 (12), 16091–16107.

Liaw, A., Wiener, M., 2002. Classification and regression by RandomForest. R News 2, 18–22.

Lopes, A., Touzi, R., Nezry, E., 1990. Adaptive speckle filters and scene heterogeneity. IEEE Transactions on Geoscience and Remote Sensing 28 (6), 992–1000.

Marsett, R.C., Qi, J., Heilman, P., Biedenbender, S.H., Watson, C.M., Amer, S., Marsett, R., 2006. Remote sensing for grassland management in the arid Southwest. Rangeland Ecology & Management/Journal of Range Management Archives 59 (5), 530–540.

McInnes, W.S., Smith, B., McDermid, G.J., 2015. Discriminating native and nonnative grasses in the dry mixedgrass prairie with MODIS NDVI Time Series. IEEE Journal of Selected Topics in Applied Earth Observations and Remote Sensing 8 (4), 1395–1403.

McNairn, H., Champagne, C., Shang, J., Holmstrom, D., Reichert, G., 2009. Integration of optical and Synthetic Aperture Radar (radar) imagery for delivering operational annual crop inventories. ISPRS Journal of Photogrammetry and Remote Sensing 64 (5), 434–449.

McNairn, H., Shang, J., 2016. A review of multitemporal synthetic aperture radar (SAR) for crop monitoring. Multitemporal remote sensing. Springer, Cham, Switzerland, pp. 317–340.

McNemar, Q., 1947. Note on the sampling error of the difference between correlated proportions or percentages. Psychometrika 12 (2), 153–157.

Metz, A., Marconcini, M., Esch, T., Reinartz, P., Ehlers, M., 2014. "Classification of grassland types by means of multi-seasonal TerraSAR-X and RADARSAT-2 imagery," 2014 IEEE Geoscience and Remote Sensing Symposium, Quebec City, QC. pp. 1202–1205.

Millard, K., Richardson, M., 2013. Wetland mapping with LiDAR derivatives, radar polarimetric decompositions, and LiDAR–radar fusion using a random forest classifier. Canadian Journal of Remote Sensing 39 (4), 290–307.

Millard, K., Richardson, M., 2015. On the importance of training data sample selection in random forest image classification: a case study in peatland ecosystem mapping. Remote Sensing 7 (7), 8489–8515.

Palchowdhuri, Y., Valcarce-Diñeiro, R., King, P., Sanabria-Soto, M., 2018. Classification of multi-temporal spectral indices for crop type mapping: a case study in Coalville, UK. The Journal of Agricultural Science 156 (1), 24–36.

Pennock, D., Bedard-Haughn, A., Viaud, V., 2011. Chernozemic soils of Canada: genesis, distribution, and classification. Canadian Journal of Soil Science 91 (5), 719–747.

Qi, J., Marsett, R., Heilman, P., Bieden-bender, S., Moran, S., Goodrich, D., Weltz, M., 2002. RANGES improves satellite-based information and land cover assessments in southwest United States. Eos, Transactions American Geophysical Union 83 (51), 601–606.

Richter, R., 1997. Correction of atmospheric and topographic effects for high spatial resolution satellite imagery. International Journal of Remote Sensing 18 (5), 1099–1111.

Roch, L., Jaeger, J.A.G., 2014. Monitoring an ecosystem at risk: what is the degree of grassland fragmentation in the Canadian Prairies? Environmental Monitoring and Assessment 186 (4), 2505–2534.

Salehi, B., Daneshfar, B., Davidson, A.M., 2017. Accurate crop-type classification using multi-temporal optical and multi-polarization SAR data in an object-based image analysis framework. International Journal of Remote Sensing 38 (14), 4130–4155.

Sheffield, C., Frier, D., Dumesh, S., 2014. The bees (Hymenoptera: Apoidea, Apiformes) of the prairies ecozone with comparisons to other grasslands of Canada. pp. 426–467.

Shorthouse, J.D., 2010. Ecoregions of Canada's prairie grasslands. Arthropods of Canadian grasslands (volume 1): ecology and interactions in grassland habitats. vol. 1. Biological Survey of Canada, pp. 53–81.

Smith, A.M., Buckley, J.R., 2011. Investigating Radarsat-2 as a tool for monitoring grassland in western Canada. Canadian Journal of Remote Sensing 37 (1), 93–102.

Smith, A.M., Hill, M.J., Zhang, Y., 2015. Estimating ground cover in the mixed prairie grassland of southern alberta using vegetation indices related to physiological function. Canadian Journal of Remote Sensing 41 (1), 51–66.

Society for Range Management, 1998. Glossary of terms used in range management. 4th ed.

Sonobe, R., Tani, H., Wang, X., Kobayashi, N., Shimamura, H., 2014. Random forest classification of crop type using multi-temporal Terraradar-X dual-polarimetric data. Remote Sensing Letters 5 (2), 157–164.

Strobl, C., Boulesteix, A.-L., Kneib, T., Augustin, T., Zeileis, A., 2008. Conditional variable importance for random forests. BMC Bioinformatics 9 (1), 307.

Tieszen, L.L., Reed, B.C., Bliss, N.B., Wylie, B.K., DeJong, D.D., 1997. NDVI, C3 and C4 production, and distributions in great plains grassland land cover classes. Ecological Applications 7 (1), 59–78.

Tucker, C.J., 1979. Red and photographic infrared linear combinations for monitoring vegetation. Remote Sensing of Environment 8 (2), 127–150.

Wang, Xin, Ge, L., Li, X., 2013. Pasture monitoring using SAR with COSMO-SkyMed, ENVISAT ASAR, and ALOS PALSAR in Otway, Australia. Remote Sensing 5 (7), 3611–3636.

Wang, C., Hunt, E.R., Zhang, L., Guo, H., 2013. Phenology-assisted classification of C3 and C4 grasses in the US Great Plains and their climate dependency with MODIS time series. Remote Sensing of Environment 138, 90–101.

Wang, X., VandenBygaart, A.J., McConkey, B.C., 2014. Land management history of canadian grasslands and the impact on soil carbon storage. Rangeland Ecology & Management 67 (4), 333–343.

Waske, B., Braun, M., 2009. Classifier ensembles for land cover mapping using multitemporal radar imagery. ISPRS Journal of Photogrammetry and Remote Sensing 64 (5), 450–457.

White, L., Millard, K., Banks, S., Richardson, M., Pasher, J., Duffe, J., 2017. Moving to the RADARSAT Constellation Mission: comparing synthesized compact polarimetry and dual polarimetry data with fully polarimetric RADARSAT-2 data for image classification of peatlands. Remote Sensing 9 (6), 573.

Wu, H., Li, Z.-L., 2009. Scale issues in remote sensing: a review on analysis, processing and modeling. Sensors 9 (3), 1768–1793.

Yang, X., Guo, X., Fitzsimmons, M., 2012. Assessing light to moderate grazing effects on grassland production using satellite imagery. International Journal of Remote Sensing 33 (16), 5087–5104.

Yang, X., Smith, A.M., Hill, M.J., 2017. Updating the grassland vegetation inventory using change vector analysis and functionally-based vegetation indices. Canadian Journal of Remote Sensing 43 (1), 62–78.

Zhang, H., Li, Q., Liu, J., Shang, J., Du, X., McNairn, H., Champagne, C., Dong, T., Liu, M., 2017. Image classification using rapideye data: integration of spectral and textual features in a random forest classifier. IEEE Journal of Selected Topics in Applied Earth Observations and Remote Sensing 10 (12), 5334–5349.

Zhu, Z., Wang, S., Woodcock, C.E., 2015. Improvement and expansion of the Fmask algorithm: cloud, cloud shadow, and snow detection for Landsats 4–7, 8, and Sentinel 2 images. Remote Sensing of Environment 159 (Suppl C), 269–277.